In vitro evaluation of biomimetic chitosan–calcium phosphate scaffolds with potential application in bone tissue engineering

2013 Biomed. Mater. 8 025002

(http://iopscience.iop.org/1748-605X/8/2/025002)

Biomed. Mater. **8** (2013) 025002 (10pp) doi:10.1088/1748-6041/8/2/025002

In vitro evaluation of biomimetic chitosan–calcium phosphate scaffolds with potential application in bone tissue engineering

C E Tanase[1,2,4], A Sartoris[3], M I Popa[1,4], L Verestiuc[2], R E Unger[3,4] and C J Kirkpatrick[3]

[1] Faculty of Chemical Engineering and Environmental Protection, 'Gheorghe Asachi' Technical University of Iasi, D Mangeron Blvd, 700050 Iasi, Romania
[2] Faculty of Medical Bioengineering, Grigore T Popa University of Medicine and Pharmacy, 9-13 Kogalniceanu Street, 700454 Iasi, Romania
[3] Institute of Pathology, REPAIR Lab, Johannes Gutenberg University, D-55101 Mainz, Germany

E-mail: etanase@tuiasi.ro, runger@uni-mainz.de and mipopa@tuiasi.ro

Received 12 September 2012
Accepted for publication 10 December 2012
Published 23 January 2013
Online at stacks.iop.org/BMM/8/025002

Abstract

This work reports on the physicochemical properties and *in vitro* cytotoxicity assessment of chitosan–calcium phosphate (Cs–CP) scaffolds for bone tissue engineering, which were synthesized by a novel biomimetic co-precipitation method. X-ray diffraction (XRD) along with scanning electron microscopy (SEM) analysis confirmed the porous morphology of the scaffolds and the amorphous nature of the inorganic phase with different crystallite sizes and the formation of various forms of calcium phosphate. Compressive mechanical testing revealed that the Young's modulus of the biomaterials is in the range of human trabecular bone. *In vitro* tests were performed on the biomaterials for up to 14 days to study the behavior of the osteoblast-like human cell line (MG63), primary human osteoblasts (HOS) and human dermal microvascular endothelial cells (HDMEC). The cytotoxicity was evaluated by the MTS assay for cell metabolism and the detection of membrane integrity (lactate dehydrogenase-LDH release). An expression of the vascular endothelial growth factor (VEGF) in the cell supernatants was quantified by ELISA. Cell viability gave values close to untreated controls for MG63 and HOS, while in the case of HDMEC the viability after 2 weeks in the cell culture was between 80–90%. The cytotoxicity induced by the Cs–CP scaffolds on MG63, HOS and HDMEC *in vitro* was evaluated by the amount of LDH released, which is a sensitive and accurate marker for cellular toxicity. The increased levels of VEGF obtained in the osteoblast culture highlights its important role in the regulation of vascularization and bone remodeling. The biological responses of the Cs–CP scaffolds demonstrate a similar proliferation and differentiation characteristics of the cells comparable to the controls. These results reveal that biomimetic Cs–CP composite scaffolds are promising biomaterials for bone tissue engineering; their *in vivo* response remains to be tested.

(Some figures may appear in colour only in the online journal)

[4] Authors to whom any correspondence should be addressed.

1. Introduction

The treatment and reconstruction of bone defects remains a major challenge for bone tissue engineering. Patients who suffer from bone defects, from high-energy traumatic events, bone resection (tumour or infection) or bone-related diseases, encounter problems due to the lack of an ideal bone scaffold [1]. The bone graft substitute market was valued at $1.9 billion in 2010 and is forecasted to reach $3.3 billion in 2017, with a compound annual growth rate of 8.3% [2]. Treatment options may include autografts, allografts and xenografts [3]. Nevertheless, the use of autografts may enhance post-operative donor site morbidity [4]. Allografts or xenografts may elicit an immune response, disease transmission or implant rejection [5, 6]. Thus, the need for bone substitute scaffolds in various clinical circumstances and the limited availability of suitable bone grafts are the driving forces for the development of tissue engineering approaches to bone repair [7]. To overcome the aforementioned limits of the autogenous and allogenic bone grafts, an increasing interest has arisen in developing new synthetic bone scaffolds. Several approaches such as sol–gel technology [8], selective laser sintering [9], electrospinning, mineralization and biomimetic methods [10, 11] in addition to many others are used for bone regeneration with the common objective to regenerate bone defects and restore the lost function. Furthermore, tissue engineering scaffolds can also be integrated into the surrounding tissue, resulting in a seamless transition between the two. This could prevent stress shielding and resorption of the healthy adjacent bone. These advantages can be mostly attributed to the development of biomimetic scaffolds. The use of biomimetic methods implies an artificial design scaffold that mimics certain advantageous features of the natural extracellular matrix to facilitate cell recruiting/seeding, adhesion, proliferation, differentiation and tissue neogenesis [12, 13]. The design of biomimetic materials represents an attempt to obtain materials with the ability to induce specific cellular responses and direct new tissue formation mediated by specific interactions.

Recently, three-dimensional biodegradable scaffolds, based on natural polymer-polysaccharides or proteins, have become a target of interest in the field of bone tissue engineering [14, 15]. Scaffolds play an important role in tissue engineering by guiding new tissue growth *in vivo* and *in vitro*. They act as a matrix for the anchorage of cells, stimulate specific cellular responses, are carriers of growth factors and are also responsible for the retention of cells in the defect that is to be filled [16]. Natural polymers often possess highly organized structures which can guide cells to grow at various stages of development. They may also stimulate an immune response at the same time [17] and contain similar structural groups to natural extra-cellular components. One of the most common biopolymers used for different biomedical applications, including bone tissue engineering, is chitosan (Cs) [18]. Cs is a linear polysaccharide, composed of glucosamine and N-acetyl glucosamine units linked by β (1–4) glycosidic bonds. Cs is considered a suitable material for biomedical applications due to its properties such as tissue compatibility, bioresorbability, antibacterial activity and haemostatic characteristics [19]; its degradation products are non-toxic, non-immunogenic, non-carcinogenic [20] and allow osteoconduction due to its porous structure [21]. Although polymeric materials alone have revealed some positive results for bone regeneration [22, 23], efforts have been made to improve and stimulate the bone response by mixing them with bone-like apatite or calcium phosphate ceramics [24–26]. Calcium–phosphate (CP) ceramics are a frequent choice and have consistently demonstrated excellent cellular and tissue responses *in vitro* and *in vivo*. The bioactivity of these ceramics has been attributed to the similarity of their composition and structure with the mineral phase of the bone [27]. Studies have demonstrated that CP materials have superior stability and *in vivo* osteogenic properties compared with autologous bone grafts [28, 29]. CP ceramics are widely used as bone substitute materials due to their osteoconductive and biocompatible properties, chemical structures similar to bone minerals, their stability in fluids and human tissue and have been used as graft materials for bone repair, augmentation and substitution [30–32]. It is well known that CP enhances osteoconductivity and extends the degradation rate of the scaffolds [33, 34]. Additionally, it has been demonstrated that CP ceramics induce bone marrow mesenchymal stem cell attachment, proliferation and differentiation [35, 36].

We reported previously that the formation of CP crystals on biopolymer fibres, without the use of any organic solvents, using an *in situ* biomimetic co-precipitation method suggested a high potential use of these biomaterials in bone tissue regeneration [37, 38]. However, before the *in vivo* evaluation of a biomaterial, it is of the upmost importance to evaluate its *in vitro* properties, such as the mitochondrial activity measured via the MTS assay, the membrane integrity determined by the LDH assay and an expression of the VEGF in the cell supernatants over a period of time, the latter being a major growth factor for vascularization. The objective of this research was to evaluate the cellular viability/cytotoxicity, an expression of differentiation and the proliferation markers of different cell types that are relevant for bone regeneration (MG63—osteoblast-like human cell line, HOS—primary human osteoblasts and HDMEC—human dermal microvascular endothelial cells) [39, 40].

2. Materials and methods

All chemicals were obtained from Sigma unless otherwise indicated.

2.1. Scaffold preparation

Cs–CP disks 10 mm in diameter and 1.5 mm thick were used in this study. The scaffolds *were prepared as previously reported* [37] by precipitation of CPs from its precursors ($CaCl_2$, NaH_2PO_4) on a Cs matrix, in the presence of NH_4OH. Briefly, an aqueous solution of $CaCl_2$ (40 wt%) and an aqueous solution of NaH_2PO_4 (25 wt%) were slowly added to a Cs solution (1 wt% in HCl 1.5 wt%) and homogenized; the pH was adjusted to 7.0 with an aqueous solution of NH_4OH

(25 wt%) and maintained for 24 h. Subsequently, the obtained mixture was washed with ultra-pure water until a neutral pH was reached and then dried at 37 °C in disk shapes. Various formulations were prepared in which different overall Cs concentrations were used, Cs–CP1—19.83% and Cs–CP2—65.74% respectively, while keeping the theoretical Ca/P ratio constant at 1.65 (similar to bone composition). The scaffolds were sterilized with a diluted ethanol solution (70%) for 15 min, followed by intensive washing in sterile phosphate buffer saline (PBS).

2.2. Scaffold characterization

2.2.1. Scanning electron microscopy. A Tescan-Vega microscope was used to observe the cross-sectional morphology of the scaffolds. All samples were coated with gold and the analysis was performed at an accelerating voltage of 30 kV.

2.2.2. X-ray diffraction (XRD) and energy-dispersive x-ray spectroscopy. XRD (XRD-6000 SHIMADZU) was carried out to determine the crystal phases of the scaffolds using monochromatic CuK_α radiation at 40 kV. An estimate of bone apatite average crystallite size, was calculated [41, 42] from Scherrer's equation (1):

$$L = \frac{k\lambda}{\beta \cos\theta} \tag{1}$$

where L denotes the average crystallite size, λ represents the x-ray radiation wavelength (0.154056 nm), k is a constant related to the crystallite shape and is approximately equal to unity, β which is experimentally measured, is the full width of the peak at half of the maximum intensity (rad). The crystallite size of the Cs–CP scaffolds (L), from the main peaks 002 and 112 reflection from the XRD pattern, is calculated by Scherrer's equation to compare the scaffolds with pure CP synthesized in the same condition as the composite scaffolds. At the same time the crystallinity of the Cs–CP scaffolds was evaluated from XRD data using the following equation (2):

$$\beta_m \times 3\sqrt{X_C = K_A} \tag{2}$$

where X_C is the crystallinity degree, β_m the full width of the peak at half intensity of 002 or 112 reflection in (2θ degree), K_A is a constant set at 0.24 [43]. An EDX-VEGA II LSH//TESCAN instrument was used to study the chemical composition of the samples.

2.2.3. Mechanical properties. The mechanical behavior of the scaffolds (average diameter 6 mm, average length 10 mm) was tested under static compression force, with a Zwick /Z005 mechanical testing instrument. The compressive modulus (or Young modulus) of the scaffolds was calculated from the plot of the force versus the material strain. Three scaffolds for each composition were tested and the measurements are reported as an average of these values.

2.3. Biocompatibility in vitro

2.3.1. Cells, culture conditions and scaffold seeding. MG63 cells (ATCC, Rockville, MD) were cultured in DMEM (Gibco) + 10% fetal bovine serum (Invitrogen) + 2 mMGlutamax I (Life Technologies) + 100 U/100 mg mL^{-1} Penicillin/Streptomycin. The HOS cells were isolated as described [44, 45]. The HOS cells were harvested exclusively from excess bone tissue obtained during the contouring procedures of iliac crest bone transplant operations for use in extensive reconstruction procedures of the facial skeleton. Bone cells were obtained and processed in accordance with local ethical regulations.

HOS cells were cultured in a medium of DMEM 4500 mg L^{-1} glucose +10%fetal bovine serum +2mMGlutamax I + 100U/100 mg mL^{-1} Penicillin/Streptomycin+75 mg L^{-1} ascorbic acid.

HDMECs were isolated from the juvenile foreskin as already described [46] and cultivated in an endothelial cell basal medium MV (Promo Cell) supplemented with a 15% fetal bovine serum, Penicillin/Streptomycin (40 units Penicillin mL^{-1}), 40 μg Streptomycin sulphate mL^{-1}, Invitrogen, sodium heparin (10 $\mu g\, mL^{-1}$) and a basic fibroblast growth factor (bFGF, 2.5 ng mL^{-1}) in a humidified atmosphere at 37 °C (5% CO_2). HOS and HDMEC cells were used until passage 4 and MG63 as previously described.

The cells were seeded onto the Cs–CP scaffolds at a density of 6.0×10^4 cells mL^{-1} in a 24-well plate (Cellstar®, Greiner Bio-one) and cultivated for different periods of time up to 14 days. Standard 24-well tissue culture plates (polystyrene) were used as a control surface. Cells were maintained under standard cell culture conditions (5% CO_2, 95% humidity and 37 °C). At predetermined times the medium was changed and collected (stored at −20 °C) in order to carry out further analysis. An expression of the VEGF and the LDH activity from supernatants were analyzed by ELISA.

2.3.2. Cytotoxicity assays. MTS conversion assay (Promega, Madison, WI). CellTiter 96®Aqueous One Solution Cell Proliferation assay was used to study cell viability. The metabolic cell activity (an indirect measure of cytotoxicity) was measured by the conversion of MTS to formazan, which can be photometrically detected. MTS was mixed with fresh medium at the ratio 1:5 and added to the cells for 1.5 h. The cells were placed in a CO_2 incubator at 37 °C. After the incubation time the supernatants were transferred to a new microplate and the optical density was measured photometrically at 492 nm.

The percentage of cell viability was calculated according to the following equation:

$$\%\ \text{Cell viability} = \frac{\text{Abs}_{\text{sample}}}{\text{Abs}_{\text{control}}} \times 100 \tag{3}$$

where $\text{Abs}_{\text{sample}}$ is the absorbance of cells tested with various formulations and $\text{Abs}_{\text{control}}$ is the absorbance of control cells (incubated with cell culture media only).

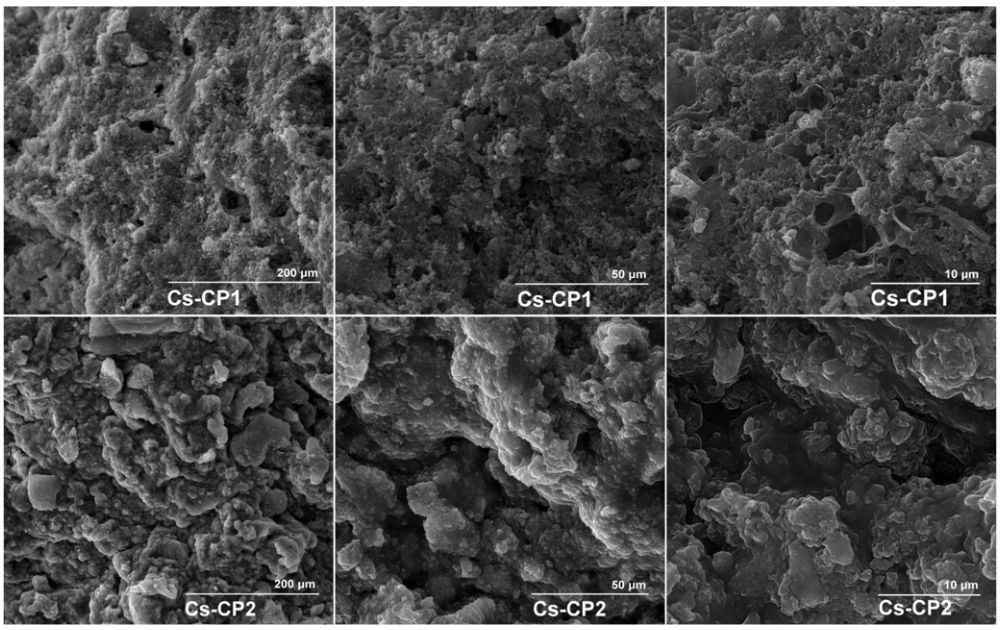

Figure 1. SEM micrographs of the cross-section in Cs–CP1 and Cs–CP2 scaffolds.

2.3.3. LDH activity assay (Promega, Madison, WI). The CytoTox 96® Non-Radioactive Cytotoxicity assay was performed following the manufacturer's protocol. This assay measures the LDH activity in the cell culture supernatants. Briefly, 50 μL of supernatants from all samples were transferred to a new microplate and 50 μL of the LDH substrate mix was added to each well. The enzymatic reaction was carried out for 30 min in the dark at room temperature and stopped by the addition of 50 μL of Stop Solution (0.2 g L^{-1} KH_2PO). The optical density was measured at 492 nm against a blank sample (a medium without cells with a LDH substrate mix and stop solution). The cells were seeded in 24 well plates (Cellstar®, Greiner Bio-one). The cells were then in contact for 24, 48 and 72 h with the Cs–CP scaffolds; after these times the supernatant was used to determine the membrane integrity determined by the LDH assay. LDH release in each sample was calculated as a percentage of the total LDH amount of the cells compared to the untreated control.

2.3.4. VEGF quantification. For each time, three samples were taken. The VEGF was quantified by ELISA using the human VEGF DuoSet (R&D Systems, Minneapolis, MN) according to the manufacturer's protocol. The VEGF value for comparisons was represented as the accumulation of the total to that particular time of all the previous values i.e. accumulated from the various measurements performed on the medium at medium change. The culture medium was used as blank.

2.3.5. Cell imaging. Confocal laser scanning microscopy (CLSM) was used to study the morphology, viability and distribution of the cells in the scaffolds. To visualize the cell nucleus using fluorescence, Vectashield-DAPI (4,6-diamino-2-phenylindole) (Vector Laboratories, CA) was used. This fluoresces bright blue when it binds selectively to double stranded DNA. The viability of the cells in the Cs–CP scaffolds were imaged using a fluorogenic substrate, calcein-acetoxymethyl ester (Calcein AM, Molecular Probes). Calcein AM is hydrolyzed into fluorescent products that are retained by the cells with an intact plasma membrane (green fluorescence).

Table 1. The formulation of Cs–CP scaffolds and a brief presentation of their characteristics.

Characteristics	Samples	Cs–CP1	Cs–CP2
Elemental composition	Cs (%)	19.83	65.74
EDX	Ca/P ratio	1.52	1.73
Solution retention at 24 h (%)	PBS	136	167
PBS-Human	Albumin	188	158

2.4. Statistics

A statistical evaluation of the data was performed using an SPSS 10 statistical package. One-way analysis of variance (ANOVA) was employed to assess the statistical significance of results at a probability of error of 5% (*), 1% (**) and 0.1% (***). Data are from three replications of each experiment and are reported as mean $\pm$ SD.

3. Results and discussion

3.1. Scaffold characterization

Two different formulations were prepared with various overall Cs concentrations and their characteristics are presented in the table 1.

Cs–CP scaffolds were characterized by SEM, XRD and compression testing. The SEM morphology and the microstructures of the cross-sectional areas of both scaffolds are shown in figure 1. The Cs–CP scaffolds showed a structure

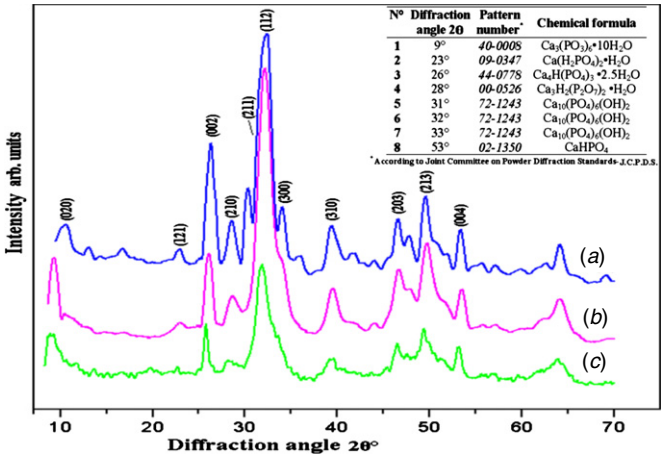

Figure 2. XRD diffractograms of (*a*) CP, (*b*) Cs–CP1, (*c*) Cs–CP2.

of irregular interconnected pores with variability in the pore size distribution and a homogeneous microstructure (Cs–CP1). With an increasing concentration of Cs in the scaffold (Cs–CP2), the pore size decreased and the polymer matrix included inorganic crystals as shown in figure 1.

The XRD results of the composite scaffolds and CP are shown in figure 2. According to the Joint Committee Powder Diffraction Standards (JCPDS), different phases are identified in the composite scaffolds, due to the CP produced by precipitation from its precursors ($CaCl_2$ and NaH_2PO_4), such as tri-calcium phosphate, dicalcium phosphate hydroxyapatite and so on, all of them having recognized properties in development of the new bone tissue [32]. In table 2 the values of crystallite size and crystallinity for the main peaks 002 and 112 reflection from the XRD pattern. The values found for crystallite size are in the range of bone apatite crystallites [47–49] and are presented. Several reports show that small crystallite domains result in a better contact reaction and stability at the interface between the CP and the natural bone as well as the promotion of early bone in-growth [50, 51].

Furthermore, the physiological temperature used in the synthesis of the prepared scaffolds resulted in the formation of crystal sizes in the range of adult human bone (∼10 nm) [32], consequently these composite scaffolds may be a good candidate for this type of application. The crystallinity values were found to be below 1, indicating a low crystallinity, which is similar to that found in biological apatites [52]. The results of mechanical testing are shown in table 2. The formulation with the lowest amount of Cs (Cs–CP1), corresponds to the highest Young modulus (140.63 MPa), followed by a composite with the highest amount of chitosan (Cs–CP2) and a lower Young modulus (69.40 MPa).

The values obtained for these scaffolds are in the range of human trabecular bone [53].

3.2. Biocompatibility in vitro

3.2.1. Cytotoxicity of the scaffolds—MTS measurement. The MTS tetrazolium compound is reduced by cells into a colored formazan product that is soluble in a tissue culture medium. The quantity of the formazan product as measured at 492 nm is directly proportional to the number of living cells in a culture. To examine the cytotoxicity of Cs–CP composites, these materials were incubated with different cell types MG63, HOS and HDMEC for up to 336 h and the cell viability (control set at 100% cell viability) was investigated by MTS assay. Figure 3(*a*) shows that Cs–CP composites did not have any effect on the viability of the MG63, while for a HOS and HDMEC culture the values of cell viability after 336 h presents a slight decrease, ranging between ∼80 and 90%. Our data are consistent with other previous investigations [54, 55]. Regardless of the cell type used, the cell viability was comparable to the control. The results indicate that all three cell types are viable on Cs–CP composite scaffolds.

3.2.2. LDH release. The numbers of nonviable cells were estimated by the colorimetric method using a CytoTox 96® Non-Radioactive Cytotoxicity Assay kit. The assay measures the release of LDH, which is a stable cytosolic enzyme that is released into the culture medium from cells with a damaged plasma membrane, resulting in the conversion of a tetrazolium salt (INT) into a red formazan product. The concentration of the dye is proportional to the number of dead cells. The results shown in figure 4(*a*) indicate the LDH release into the supernatant for the MG63 culture. The data reveal that the LDH did not increase significantly, indicating that the Cs–CP scaffolds do not exert any significant degree of cytotoxicity. The results of the membrane integrity determined by the LDH assay, for HOS and HDMEC culture (figures 4(*b*) and (*c*)) indicate a difference between the Cs–CP scaffolds investigated, which correspond with the results of the viability test. Thus, in the case of the HOS, the Cs–CP1 scaffold shows over the 72 h period approximately 7% to 13% cell lysis of the population, compared to values of maximally 3.9% for the Cs–CP2 scaffold (figure 4(*b*)). Figure 4(*c*) demonstrates clearly that endothelial cells (HDMEC) on the Cs–CP1 scaffold suffer from approximately 10% to 20% cell lysis, which is markedly higher than for Cs–CP2, which shows minimal toxic effects.

3.2.3. VEGF quantification. The effect of the Cs–CP composite scaffolds on VEGF gene expression was investigated in MG63, HOS and HDMEC cells. VEGF is produced and secreted by a variety of cell types [56] and evidence exists that osteoblasts produce and secrete VEGF in response to various physiological agents [57, 58].

VEGF is one of the most powerful pro-angiogenic growth factors and exerts well-established actions on endothelial cells, as well as a proposed direct effect on osteoblast functions [59, 60]. Evidence that VEGF directly stimulates migration and differentiation of primary human osteoblasts has been reported [61]. Furthermore, from *in vivo* studies, VEGF levels have been suggested to be a significant factor for monitoring biological and pathological tissue reaction to implants or transplants [62–64]. In this study, the VEGF profile investigated by the MG63 cells in contact with Cs–CP scaffolds (figure 5(*a*)) indicated small, though statistically significant differences from the untreated control, but overall the trend was similar. Thus, although MG63 cells on the Cs–CP1 scaffold showed slightly lowered VEGF production over the 14 day

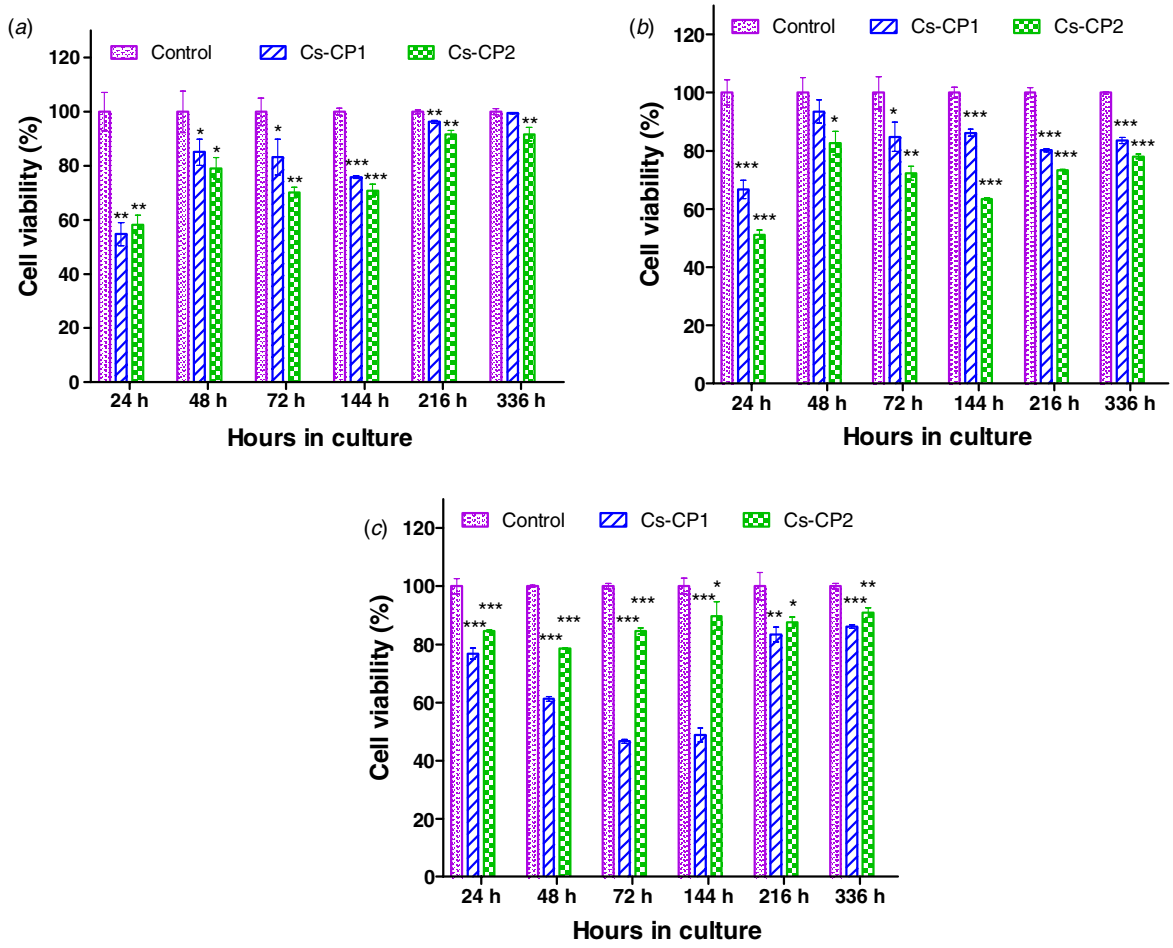

Figure 3. Mitochondrial activity measured via the MTS assay for A-MG63, B-HOS and C-HDMEC culture at different times for Cs–CP composites. Data are depicted as a percentage of the untreated control. Triplicates were performed and the data represent means ± SD. $^{*}P < 0.05$, $^{**}P < 0.01$ and $^{***}P < 0.001$ compared to the untreated control.

Table 2. Average crystallite size and crystallinity of the CP formed into Cs matrix of the scaffolds.

Batch	Ca/P ratio	FWHM (002)	FWHM (112)	Crystallite size, L_{002} (nm)	Crystallite size, L_{112} (nm)	Crystallinity $X_{C\,002}$	Crystallinity $X_{C\,112}$	Young Modulus (MPa)
Bone	1.67	–	–	∼10[a]	–	–	–	40–400
Cs–CP1	1.52	0.96	1.75	8.40	4.66	0.62	0.51	140.63
Cs–CP2	1.73	1.21	1.96	6.63	4.15	0.58	0.49	69.40

[a]According to [49].

study period, neither scaffold elicited any massive change in VEGF production which could be interpreted as biologically significant. Regarding the VEGF concentration from the HOS culture (figure 5(*b*)) the VEGF values were significantly higher on both scaffold types compared to the untreated control.

Overall these data indicate that the Cs–CP scaffolds did not markedly affect the production and secretion of VEGF. Furthermore, the scaffolds could be a good substrate concerning the VEGF production by HOS. In the HDMEC culture, no VEGF was detected.

The results obtained for the osteoblast (MG63 and HOS) culture on Cs–CP scaffolds were consistent with previous investigations, as osteoblasts were the predominant source of VEGF [65]. The up-regulation of genes coding for potent angiogenic inducers, like VEGF, acting synergistically *in vivo* and *in vitro* [66] suggests that *in vivo* Cs–CP scaffolds may be expected to support vascularization, although the latter still has to be proven in separate studies.

3.2.4. Scaffold morphology. Tests on cell viability and proliferation on Cs–CP scaffolds were performed before the CLSM study. Calcein AM was used to stain the cells cultured for 168 h (figure 6) because at this time the cells are well distributed on the Cs–CP scaffolds. The cells were evenly distributed in the Cs–CP scaffolds and appeared to bridge over the pores. Moreover, they showed a morphology similar to cells grown under normal culture conditions. At the final time point

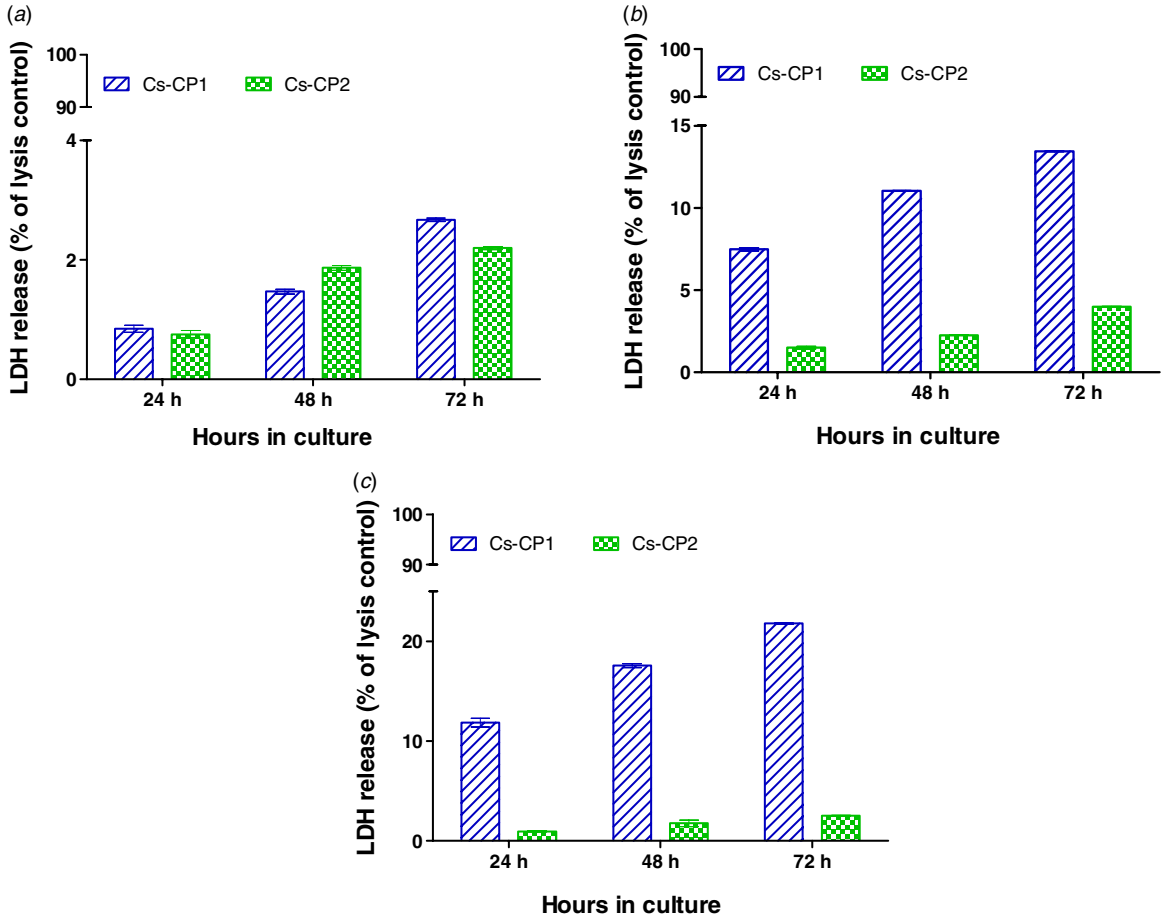

Figure 4. Membrane integrity determined by the LDH assay for A-MG63, B-HOS and C-HDMEC culture at different time points for Cs–CP composites. Data are depicted as percentages of the total LDH amount of the cells. Triplicates were performed and the data represent means ± SD.

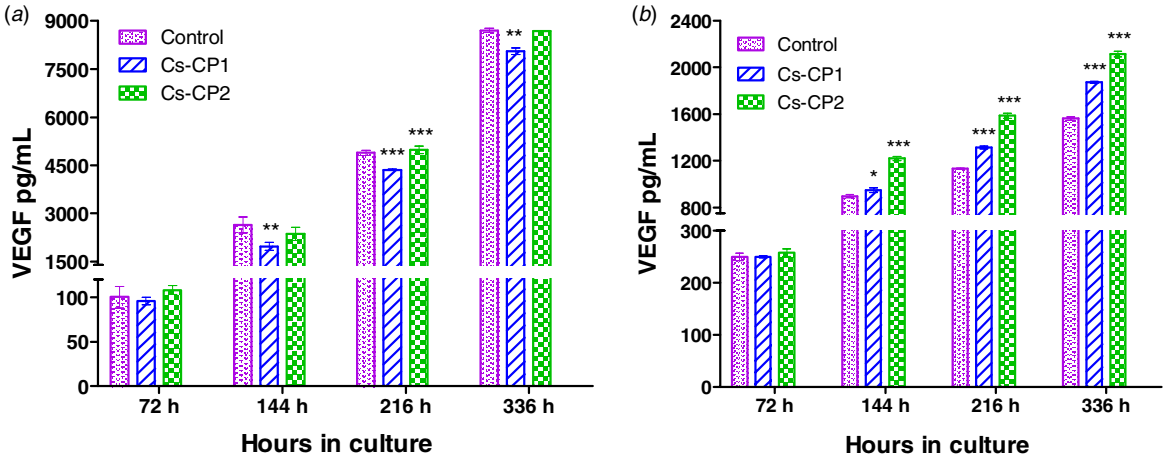

Figure 5. VEGF release profile at different times for Cs–CP composites in MG63 culture. A shows the results for MG-63 cells and B are the results for HOS cells. Triplicates were performed and the data represent means ± SD. $^{*}P < 0.05$, $^{**}P < 0.01$ and $^{***}P < 0.001$ compared to the untreated control.

for cell culture (336 h), a live staining (calcein AM) and DAPI counterstain was performed on whole samples (figure 7). The samples chosen for staining were Cs–CP scaffolds in a culture with MG63 due to the fact that cell viability was highest in this cell type compared to the HOS and HDMEC culture. Calcein AM staining (figures 7(*a*) and (*b*)) confirmed that the MG63 cells colonized the Cs–CP scaffolds to a high degree.

Staining of the nuclei of MG63 after 336 h of culture was performed by DAPI, a reagent that specifically binds to DNA regions rich in thymine, giving a blue staining

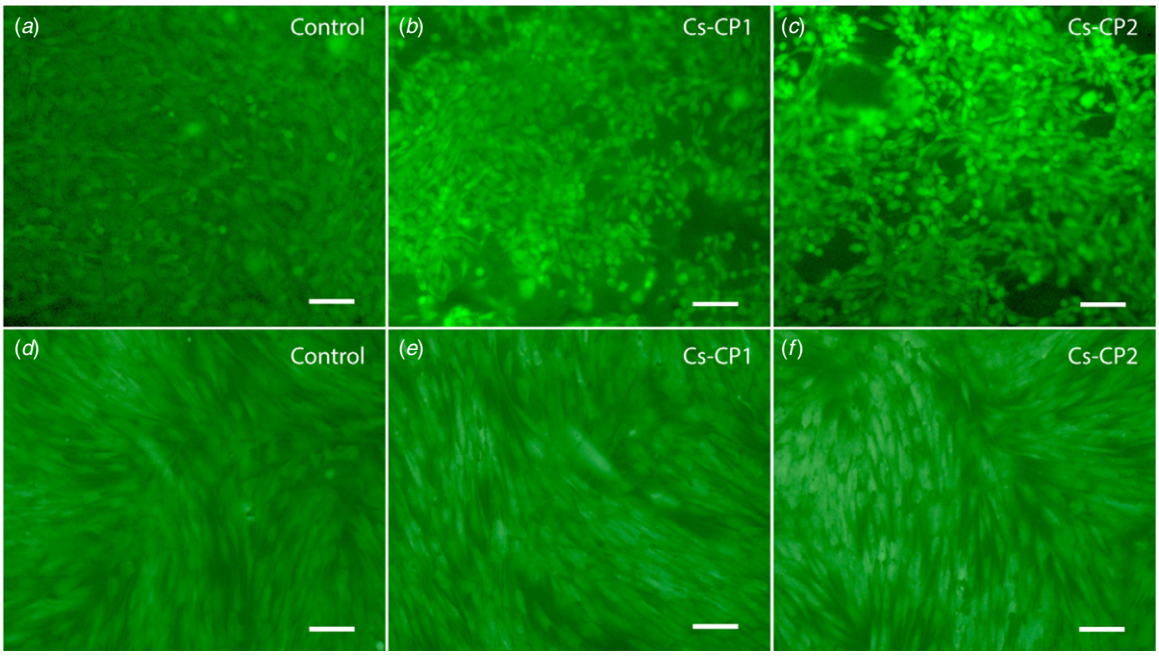

Figure 6. Fluorescent microscopy (Calcein AM) for Cs–CP scaffolds at 168 h cell cultured with MG63 ((*a*) Control, (*b*) Cs–CP1 and (*c*) Cs–CP2) and HDMEC (*d*) Control, (*e*) Cs–CP1 and (*f*) Cs–CP2) (scale bar is 100 μm).

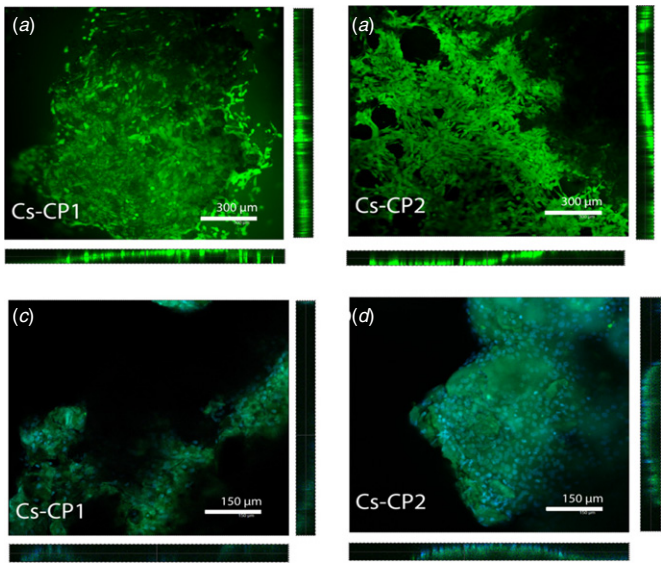

Figure 7. Confocal laser scanning microscopy imaging and cross-sections of an image series of MG63 stained with Calcein AM ((*a*) Cs–CP1 and (*b*) Cs–CP2) for viable cells (green) and DAPI staining of the nuclei of MG63 cells ((*c*) Cs–CP1 and (*d*) Cs–CP2). The images were taken at 336 h after cell seeding and demonstrate widespread colonization of the scaffolds and lack of toxicity even after 14 days of cultivation on the biomaterials.

reaction (figures 7(*c*) and (*d*)). The results indicate that the composite scaffolds Cs–CP presents a good potential as a substrate for the adhesion, spreading and proliferation of cells relevant for bone regeneration. Naturally, the next step of the investigation (to be performed in a separate *in vivo* study) is to elucidate whether these positive results *in vitro* can be confirmed in the complexity of the implantation situation, in which inflammatory processes come to bear.

4. Conclusions

In this work, *in vitro* biocompatibility studies were performed for Cs–CP composite scaffolds synthesized via a biomimetic co-precipitation method. The XRD results showed that composites based on Cs and CP contain different forms of calcium phosphate (CP), with various Ca/P ratios and crystallite size as well as crystallinity similar to bone tissue. The Cs–CP composite scaffolds showed mechanical properties in the range of human trabecular bone. Cell viability studies were performed using human cells of osteoblast origin (MG63, HOS) as well as microvascular endothelial cells (HDMEC). From assays for mitochondrial activity and detection of membrane integrity, data are presented that support the possible application of Cs–CP scaffolds to bone and wound tissue engineering. Assessment of VEGF expression (secreted protein) was performed and the results suggest that Cs–CP scaffolds could be a good substrate with respect to the support of vascularization. The morphology of cells visualized by phase contrast microscopy and immunofluorescent staining investigated by CLSM clearly demonstrated that cells adhered to the biomaterials, and over a period of 14 days gave widespread colonization. Therefore, this study underscores Cs–CP composite scaffolds as a promising biomaterial for bone tissue engineering. Animal studies remain to be carried out in order to evaluate the effect of the Cs–CP scaffold on bone regeneration *in vivo*.

Acknowledgments

This paper was realized with the support of the BRAIN project—'Doctoral scholarships as an investment in intelligence', financed by the European Social Fund and the Romanian Government.

References

[1] Schroeder J E and Mosheiff R 2011 Tissue engineering approaches for bone repair: concepts and evidence *Injury* **42** 609

[2] GlobalData 2011 Bone graft substitutes—global pipeline analysis, competitive landscape and market forecast to 2017 GBDT6459509

[3] Kao S T and Scott D D 2007 A review of bone substitutes *Oral Maxillofac. Surg. Clin. North Am.* **19** 513

[4] Zárate-Kalfópulos B and Reyes-Sánchez A 2006 Injertos óseos en cirugía ortopédica *Cir. Ciruj.* **74** 217

[5] Vagaska B, Bacakova L, Filova E and Balik K 2010 Osteogenic cells on bio-inspired materials for bone tissue engineering *Physiol. Res.* **59** 309

[6] Kretlow J D and Mikos A G 2008 2007 AIChE alpha chi sigma award: from material to tissue: biomaterial development, scaffold fabrication, and tissue engineering *AIChE J.* **54** 3048

[7] Frohlich M, Grayson W L, Wan L Q, Marolt D, Drobnic M and Vunjak-Novakovic G 2008 Tissue engineered bone grafts: biological requirements, tissue culture and clinical relevance *Curr. Stem Cell Res. Ther.* **3** 254

[8] Raucci M G, Guarino V and Ambrosio L 2010 Hybrid composite scaffolds prepared by sol-gel method for bone regeneration *Compos. Sci. Technol.* **70** 1861

[9] Duan B, Wang M, Zhou W Y, Cheung W L, Li Z Y and Lu W W 2010 Three-dimensional nanocomposite scaffolds fabricated via selective laser sintering for bone tissue engineering *Acta Biomater.* **6** 4495

[10] Pallab D, Santanu D and Jyotirmoy C 2012 Hydrogels and electrospun nanofibrous scaffolds of N-methylene phosphonic chitosan as bioinspired osteoconductive materials for bone grafting *Carbohydr. Polym.* **87** 1354

[11] Antonietti M and Fratzl P 2010 Biomimetic principles in polymer and material science *Macromol. Chem. Phys.* **211** 166

[12] GraysoW L, Martens T P, George M, Radisic M and Vunjak-Novakovic G 2009 Biomimetic approach to tissue engineering *Semin. Cell Dev. Biol.* **20** 665

[13] Liao S, Chan C K and Ramakrishna S 2008 Stem cells and biomimetic materials strategies for tissue engineering *Mater. Sci. Eng. C* **28** 1189

[14] Bauer T W 2007 Bone graft substitutes *Skeletal Radiol.* **36** 1105

[15] Salgado A J, Coutinho O P and Reis R L 2004 Bone tissue engineering: state of the art and future trends *Macromol. Biosci.* **4** 743

[16] Aziz N 2005 *Bone Grafts and Bone Substitutes Basic Science and Clinical Applications* (Singapore: World Scientific)

[17] Cheung H Y, Lau K T, Lu T P and Hui D 2007 A critical review on polymer-based bio-engineered materials for scaffold development *Composites* B **38** 291

[18] Muzzarelli R A A 2011 Chitosan composites with inorganics, morphogenetic proteins and stem cells, for bone regeneration *Carbohydr. Polym.* **83** 1433

[19] Muzzarelli R A A 2009 Chitins and chitosans for the repair of wounded skin, nerve, cartilage and bone *Carbohydr. Polym.* **76** 167

[20] Kim I, Y,Seo S J, Moon H S, Yoo M K, Park I Y, Kim B C and Cho C S 2008 Chitosan and its derivatives for tissue engineering applications *Biotechnol. Adv.* **26** 1

[21] Dasha M, Chiellini F, Ottenbriteb R M and Chiellini E 2011 A versatile semi-synthetic polymer in biomedical applications *Prog. Polym. Sci.* **36** 981

[22] Shin M, Yoshimoto H and Vacanti J P 2004 *In vivo* bone tissue engineering using mesenchymal stem cells on a novel electrospun nanofibrous scaffold *Tissue Eng.* **10** 33

[23] Badami A S, Kreke M R, Thompson M S, Riffle J S and Goldstein A S 2006 Effect of fiber diameter on spreading, proliferation, and differentiation of osteoblastic cells on electrospun poly(lactic acid) substrates *Biomaterials* **27** 596

[24] Pallela R, Venkatesan J, Janapala V R and Kim S K 2011 Biophysicochemical evaluation of chitosan-hydroxyapatite-marine sponge collagen composite for bone tissue engineering *J. Biomed. Mater. Res.* A **100** 486 (PMID: 22125128)

[25] Panetta J N, Gupta M D and Longaker T M 2010 Bone regeneration and repair *Curr. Stem Cell. Res. Ther.* **5** 122

[26] Jose M V, Thomas V, Xu Y, Bellis S, Nyairo E and Dean D 2010 Aligned bioactive multi-component nanofibrous nanocomposite scaffolds for bone tissue engineering *Macromol. Biosci.* **10** 433

[27] Bohner M, Galea L and Doebelin N 2012 Calcium phosphate bone graft substitutes: failures and hopes *J. Eur. Ceram. Soc.* **32** 2663

[28] Eniwumide J O, Yuan H, Cartmell S H, Meijer G J and de Bruijn J D 2007 Ectopic bone formation in bone marrow stem cell seeded calcium phosphate scaffolds as compared to autograft and (cell seeded) allograft *Eur. Cell. Mater.* **14** 30

[29] Fellah B H, Gauthier O, Weiss P, Chappard D and Layrolle P 2008 Osteogenicity of biphasic calcium phosphate ceramics and bone autograft in a goat model *Biomaterials* **29** 1177

[30] Murugan R and Ramakrishna S 2004 Bioresorbable composite bone paste using polysaccharide based nano hydroxyapatite *Biomaterials* **25** 3829

[31] LeGeros R Z 2002 Properties of osteoconductive biomaterials: calcium phosphates *Clin. Orthop. Relat.* R **395** 81

[32] Vallet-Regí M and González-Calbet J M 2004 Calcium phosphates as substitution of bone tissues *Prog. Solid State Chem.* **32** 1

[33] Wang Y, Zhang L, Hu M, Liu H, Wen W, Xiao H and Niu Y 2008 Synthesis and characterization of collagen-chitosan-hydroxyapatite artificial bone matrix *J. Biomed. Mater. Res.* A **86** 244

[34] Best S M, Porter A E, Thian E S and Huang J 2008 Bioceramics: past, present and for the future *J. Eur. Ceram. Soc.* **28** 1319

[35] Riberio C C, Barrias C C and Barbosa M A 2006 Preparation and characterisation of calcium-phosphate porous microspheres with a uniform size for biomedical applications *J. Mater. Sci. Mater.* M **17** 455

[36] Schieker M, Seitz H, Drosse I, Seitz S and Mutschler W 2006 Biomaterials as scaffold for bone tissue engineering *Eur. J. Trauma* **32** 114

[37] Tanase C E, Popa M I and Verestiuc L 2009 Chitosan-hydroxyapatite composite obtained by biomimetic method as new bone substitute *Proc. 2009 ECSIS Symp. on Advanced Technologies for Enhanced Quality of Life AT-EQUAL (Los Alamitos, CA: IEEE Computer Society)* p 42–6

[38] Tanase C E, Popa M I and Verestiuc L 2012 Biomimetic chitosan-calcium phosphate composites with potential applications as bone substitutes: preparation and characterization *J. Biomed. Mater. Res.* B **100** 700

[39] Jones J R, Tsigkou O, Coates E E, Stevens M M, Polak J M and Hench L L 2007 Extracellular matrix formation and mineralization on a phosphate-free porous bioactive glass scaffold using primary human osteoblast (HOB) cells *Biomaterials* **28** 1653

[40] Santos M I, Tuzlakoglu K, Fuchs S, Gomes M E, Peters K, Unger R E, Piskin E, Reis R L and Kirkpatrick C J 2008 Endothelial cell colonization and angiogenic potential of combined nano- and micro-fibrous scaffolds for bone tissue engineering *Biomaterials* **29** 4306

[41] Danilchenko S N, Kukharenko O G, Moseke C, ProtsenkoI Y, Sukhodub L F and Sulkio-Cleff B 2002 Determination of the bone mineral crystallite size and lattice strain from diffraction line broadening *Cryst. Res. Technol.* **37** 1234
[42] Barrett C S, Cohen J B, Faber J Jr, Jenkins R, Leyden D E, Russ J C and Predecki P K 1986 *Advances in X-ray Analysis* (New York: Plenum)
[43] Landi E, Tampieri A, Celotti G and Sprio S 2000 Densification behaviour and mechanisms of synthetic hydroxyapatites *J. Eur. Ceram. Soc.* **20** 2377
[44] Annaz B, Hing K A, Kayser M, Buckland T and Di Silvio L 2004 An ultrastructural study of cellular response to variation in porosity in phase-pure hydroxyapatite *J. Microsc.* **216** 97
[45] Koller M R, Palsson B O and Masters J R W 2001 *Human Cell Culture* (Dordrecht: Kluwer)
[46] Kirkpatrick C J, Barth S, Gerdes T, Krump-Konvalinkova V and Peters K 2002 Pathomechanisms of impaired wound healing by metallic corrosion products *Mund Kiefer. Gesichtschir* **6** 183
[47] Lundy D R and Eanes E D 1973 An x-ray line-broadening study of turkey leg tendon *Arch. Oral Biol.* **18** 813
[48] Posner A S 1969 Crystal chemistry of bone mineral *Physiol. Rev.* **49** 760
[49] Boskey A L 2002 Variations in bone mineral properties with age and disease *J. Musculoskel. Neuron Interact.* **2** 532
[50] Webster T J, Ergun C, Doremus R H, Siegel R W and Bizios R 2000 Enhanced functions of osteoblasts on nanophase ceramics *Biomaterials* **21** 1803
[51] Fathi M H and Hanifi A 2007 Evaluation and characterization of nanostructure hydroxyapatite powder prepared by sol-gel method *Mater. Lett.* **61** 3978
[52] Rusu V M, Chuen-How N, Wilke M, Tiersch B, Fratzl P and Peter M G 2005 Size-controlled hydroxyapatite nanoparticles as self-organized organic-inorganic composite materials *Biomaterials* **26** 5414
[53] Carter D R and Heyes W C 1977 The compressive behavior of bone as a two-phase porous structure *J. Bone Joint Surg. Am.* **59** 954
[54] Chesnutt B M, Viano A M, Yuan Y, Yang Y, Guda T, Appleford MR, Ong J L, Haggard W O and Bumgardner J D 2009 Design and characterization of a novel chitosan/nanocrystalline calcium phosphate composite scaffold for bone regeneration *J. Biomed. Mater. Res.* A **88** 491
[55] Xu H H and Simon C G Jr 2005 Fast setting calcium phosphate-chitosan scaffold: mechanical properties and biocompatibility *Biomaterials* **26** 1337
[56] Ferrara N 2004 Vascular endothelial growth factor: basic science and clinical progress *Endocrinol. Rev.* **25** 581
[57] Schlaeppi J M, Gutzwiller S, Finkenzeller G and Fournier B 1997 1,25-dihydroxyvitamin D3 induces the expression of vascular endothelial growth factor in osteoblastic cells *Endocrinol. Res.* **23** 213
[58] Goad D L, Rubin J, Wang H, Tashjian A H Jr and Patterson C 1996 Enhanced expression of vascular endothelial growth factor in human SaOS-2 osteoblast-like cells and murine osteoblasts induced by insulin-like growth factor: 1 *Endocrinol.* **137** 2262
[59] Li G, Cui Y X, McIlmurray L, Allen W E and Wang H 2005 rhBMP-2, rhVEGF(165), rhPTN and thrombin-related peptide, TP508 induce chemotaxis of human osteoblasts and microvascular endothelial cells *J. Orthop. Res.* **23** 680
[60] Roy H, Bhardwaj S and Yla-Herttuala S 2006 Biology of vascular endothelial growth factors *FEBS Lett.* **580** 2879
[61] Mayr-Wohlfart U, Waltenberger J, Hausser H, Kessler S, Gunther K P, Dehio C, Puhl W and Brenner R E 2002 Vascular endothelial growth factor stimulates chemotactic migration of primary human osteoblasts *Bone* **30** 472
[62] Peattie R A, Nayate A P, Firpo M A, Shelby J, Fisher R J and Prestwich G D 2004 Stimulation of *in vivo* angiogenesis by cytokine-loaded hyaluronic acid hydrogel implants *Biomaterials* **25** 2789
[63] Sanders J E, Wang Y N, Malcolm S G and Lamont S E 2003 Biomaterial mesh seeded with vascular remnants from a quail embryo has a significant and fast vascular templating effect on host implant tissue *Tissue Eng.* **9** 1271
[64] Ascencio D, Hernández-Pando R, Barrios J, Soriano R E, Perez-Guille B, Villegas F, Sanz C R, López-Corella E, Carrasco D and Frenk S 2004 Experimental induction of heterotopic bone in abdominal implants *Wound Repair Regen.* **12** 643
[65] Clarkin C E, Emery R J, Pitsillides A A and Wheeler-Jones C P 2008 Evaluation of VEGF-mediated signaling in primary human cells reveals a paracrine action for VEGF in osteoblast-mediated crosstalk to endothelial cells *J. Cell. Physiol.* **214** 537
[66] Tille J C and Pepper M S 2002 Mesenchymal cells potentiate vascular endothelial growth factor-induced angiogenesis *in vitro Exp. Cell Res.* **280** 179